Electronic Supplementary Information For:

Direct growth of h-BN multilayers with controlled thickness on noncrystalline dielectric substrates without metal catalyst

*Xiaoyan Sun,[a] Yuanfang Feng,[a] Fei Wang,[a] Peng Wang,[a] Wei Gao,[a]*and Hong Yin [a]**

[a] State Key Lab of Superhard Materials, College of Physics, Jilin University, Changchun 130012, Jilin, P. R. China.

***Corresponding authors.**

E-mail: hyin@jlu.edu.cn and gwei@jlu.edu.cn

Growth process:

a). To synthesize h-BN film on the dielectric substrate directly, we need to pretreat the substrate with rGO for forming a homogeneous rGO pristine layer fully covering the substrate surface. To achieve this objective, we take 5-10 mg of rGO powder dispersed in an aqueous sodium lauryl sulfate (SDS，85%) solution with concentration of 0.2~0.5mg/ml, stirred the mixed solution for 72 h and sonicated it for 10 h. Take the upper stable dispersion and make it evenly spread on the substrate we used. After the substrate covered with rGO fully dried, the above steps are repeated 2 times. Then the substrate was heated in Ar at 500 °C for 20 min to remove volatile impurities and enhance binding between rGO and substrate.

b). Then we weigh 500 mg of B_2O_3 powder and spread it flat in the corundum boat, and take another corundum boat to hold the previously processed quartz substrate. The position of the quartz substrate is in the middle of the boat. Then the two boats are placed in the center of the tube furnace in order, and reacted at a temperature of 850 °C for 1 h. During the reaction, the total flow of ammonia gas and argon gas is 200 sccm, of which the flow of ammonia gas is controlled at 50~100 sccm, the heating rate is 5 °C/min, and the temperature drop rate is 8.5 °C/min. After the reactions, the films are washed by 80 °C hot water twice to remove the boric acid or boron oxide residues on the surface. Schematic diagram of the CVD system is shown in Figure S1.

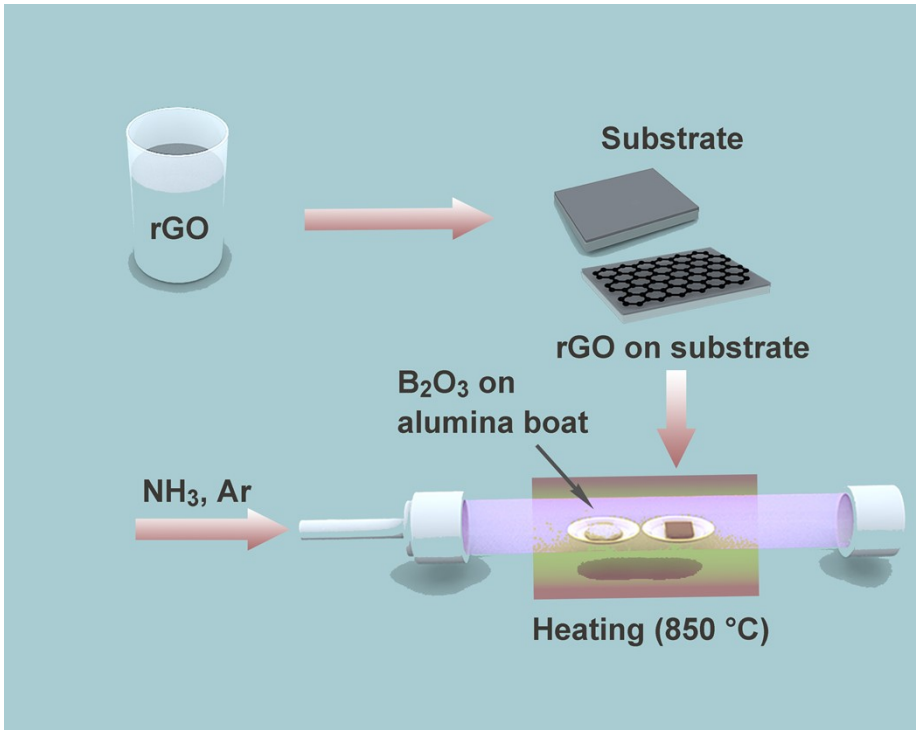

Figure S1. Schematic diagram of the CVD system used for h-BN films growth.

Characterizations:

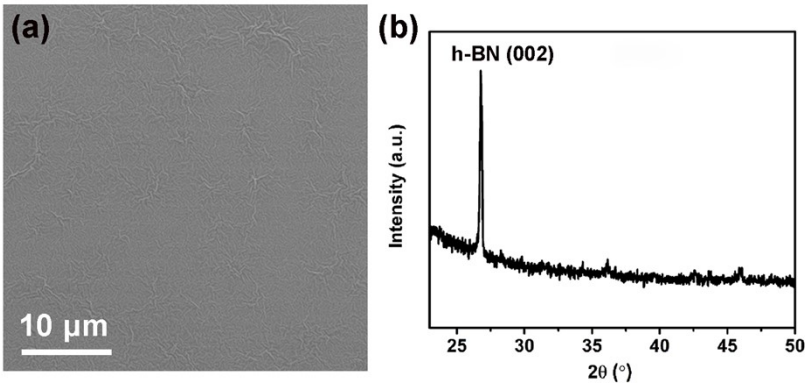

Figure S2. SEM image (a) and XRD spectrum (b) of the thin h-BN film grown on quartz.

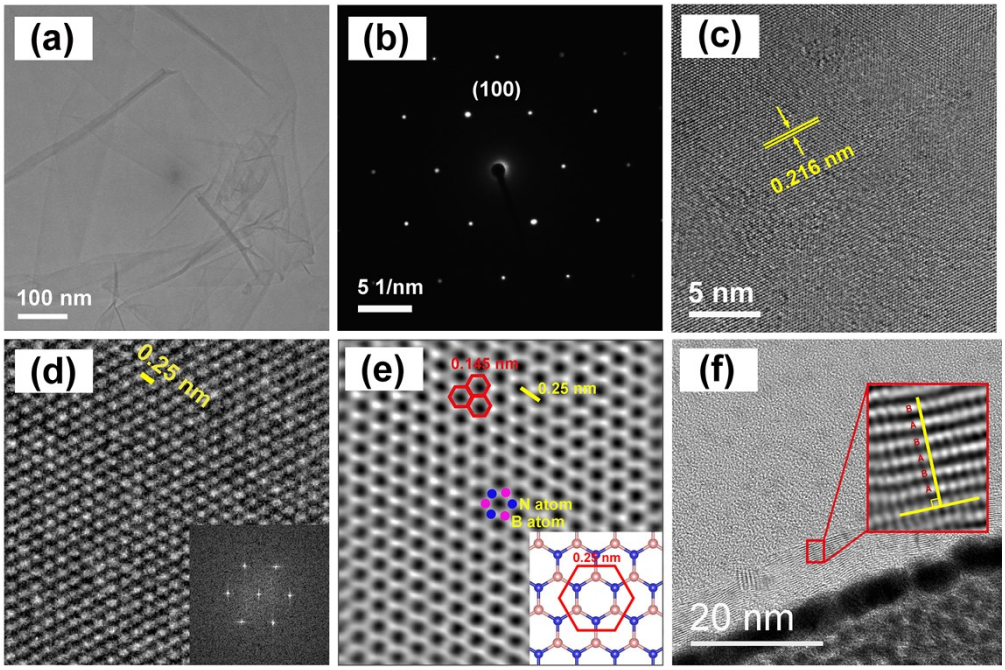

Figure S3. (a) Low-magnification TEM image of a continuous h-BN film. (b) Electron diffraction pattern of the h-BN thin film taken from a freely suspended region. (c) A typical HRTEM image obtained from (a). (d) The enlarge HRTEM image. Corresponding FFT image is shown in the inset. (e) The FFT filtered HRTEM image of the h-BN film. (f) HRTEM image of the cross-section of h-BN film. The inset is enlarged HRTEM image of the cross-section of h-BN film after Fourier filtering.

The crystal structure and crystallinity of the h-BN film were studied further using HRTEM and SAED, and the results are shown in Figure S3. The low-magnified TEM view in Figure S3a indicates the existence of a highly continuous h-BN film transferred onto the TEM grid. The existence of wrinkles mainly caused by transfer makes it easier to distinguish the presence of the thin film. In Figure S3b, the selected area electron diffraction (SAED) was taken on the smooth region of the film, which shows a unique set of six-fold symmetric diffraction pattern. This is consistent with the description of the film as a uniform single crystalline nature. As can be seen from Figure S3c, a sharp

lattice fringe with the interplanar space of 0.216 nm for (100) planes, further confirming the hexagonal single crystallinity. Corresponding high-magnified HRTEM image (Figure S3d) reveals a honeycomb structure with an interatomic distance of 0.25 nm, in good agreement with that of bulk h-BN. The fast Fourier transform (FFT) obtained from the whole image (inset of Figure S3d) shows only one set of hexagonal spots, which indicates a highly periodic h-BN structure with no differences in rotational orientation between the layers. Figure S3e is the FFT filtered HAADF-STEM image, the B and N atoms in a hexagonal network can be direct observed. The brighter spots are identified as N atoms, due to their slightly higher atomic number than B atoms, causing Z-contrast intensity variation in the HAADF images.[1] The HRTEM image focusing on the cross-section of h-BN film shows a well-defined layered structure of h-BN multilayers (Figure S3f). The enlarged HRTEM image taken at selected area after Fourier filtering directly shows an ideal "ABAB" pattern of atomic layers, white dots correspond to BN atomic pair, excellently fitting to the theoretically generated atomic arrangement of h-BN (inset of Figure S3f). Here, it is worth mentioning that when preparing cross-section samples, the presence of Pt can protect the sample surface from damage. In view of the insulating properties of quartz and h-BN, a layer of gold plating was sprayed on the sample surface for better characterization of h-BN films.

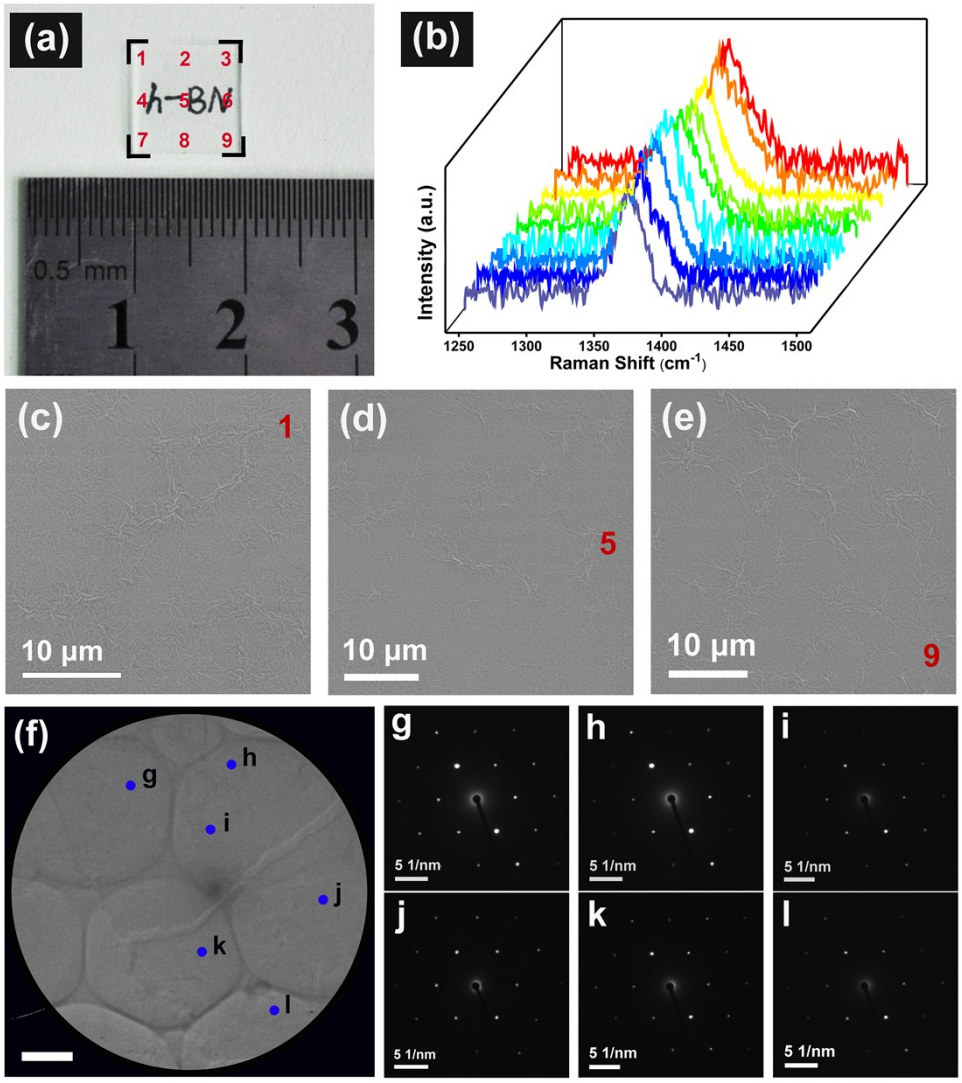

Figure S4. (a) The photo of uniform h-BN multilayers grown on quartz substrate. (b) Raman spectra of h-BN at different positions as indicated in (a). (c-e) The SEM image of h-BN at different positions as indicated in (a). (f) Low magnification image showing a continuous h-BN film on TEM grids. Scale bar is 1 μm. (g-l) The SAED pattern of the h-BN film at different positions as indicated in (f).

To study the uniformity of the CVD-grown h-BN film, the films were characterized by Raman spectroscopy. Figure S4a shows the photograph of a continuous and highly transparent h-BN film on the quartz substrate. Raman analysis was performed at nine different positions, as indicated in Figure

S4b. Each Raman peak measured at different positions on the h-BN film is located between 1369 and 1371 cm^{-1}, originating from the in-plane B-N bond stretching of h-BN, indicating that the continuous h-BN film has a uniform layer number. In addition, the FWHM has a relatively narrow distribution from 31 to 35 cm^{-1}, which is consistent with highly crystalline of h-BN directly grown dielectric substrates. As shown in Figure S4c-e, SEM images at three different positions (1, 5 and 9) demonstrate the uniformity of the surface morphology of the grown h-BN film. The uniformity of crystallinity of the grown h-BN film were also studied further using SAED. Figure S4g-l illustrates our SAED measurements at six random positions over a large area (marked by blue dots in Figure S4f). It can be seen that no significantly different crystal orientations were observed, which indicates that the SAED patterns still belonged to the same single h-BN domain over the large area. Meanwhile, the dispersion of the light spot varies with the change of the measurement area, which may be attributed to the accidental folding of h-BN layers introduced during the sample transfer process.

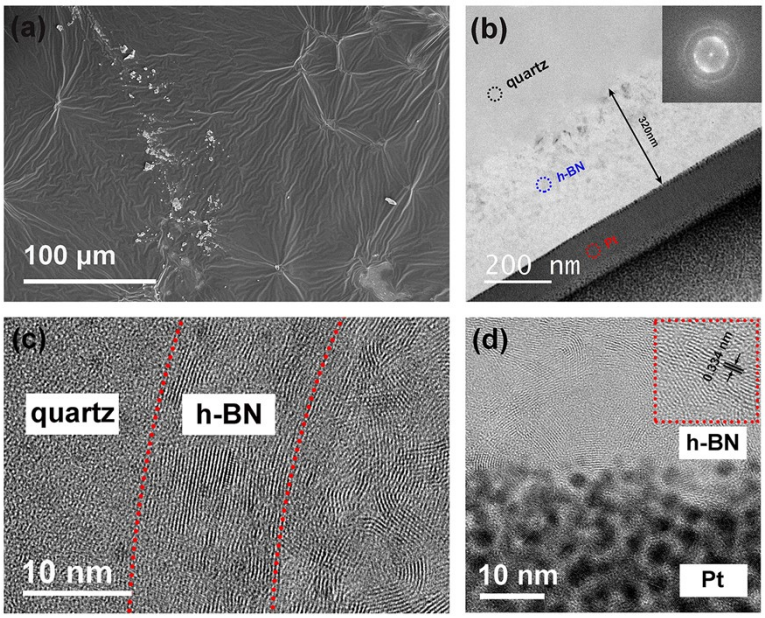

Figure S5. (a) The SEM image of the thicker h-BN films prepared with 0.5 mg/ml rGO concentration of on quartz. (b-d) Low-magnification and atomic-resolution TEM image of the cross-section of h-BN films on the TEM micro grid. The inset in (d) shows a zoom-in view of lattice fringes with a spacing of 0.334 nm.

Figure S5a shows the SEM image of the thicker h-BN film prepared with rGO at a concentration of 0.5 mg/ml, in which a uniform and continuous film can be observed with intensive wrinkles. The cross-sectional TEM image (Figure S5b) shows a thickness of about 320 nm (EDS mapping is shown in Figure S6). The corresponding electron diffraction pattern exhibit a ring-like structure with incomplete dots, suggesting a non-single crystal nature with short-range preferential orientation in the current case. Figure S5c and 5d is the high-resolution electron microscope image of the cross-section of the h-BN film, in which we can see the formation of large amounts of randomly oriented single crystal h-BN (002) domains. This is due to the fact that increasing the concentration of the precursor leads to a higher defect density of rGO layer, giving rise to an excessive increase in

the h-BN nucleation density. As a result, the nucleation of h-BN is so fast that the film forms to polycrystalline.

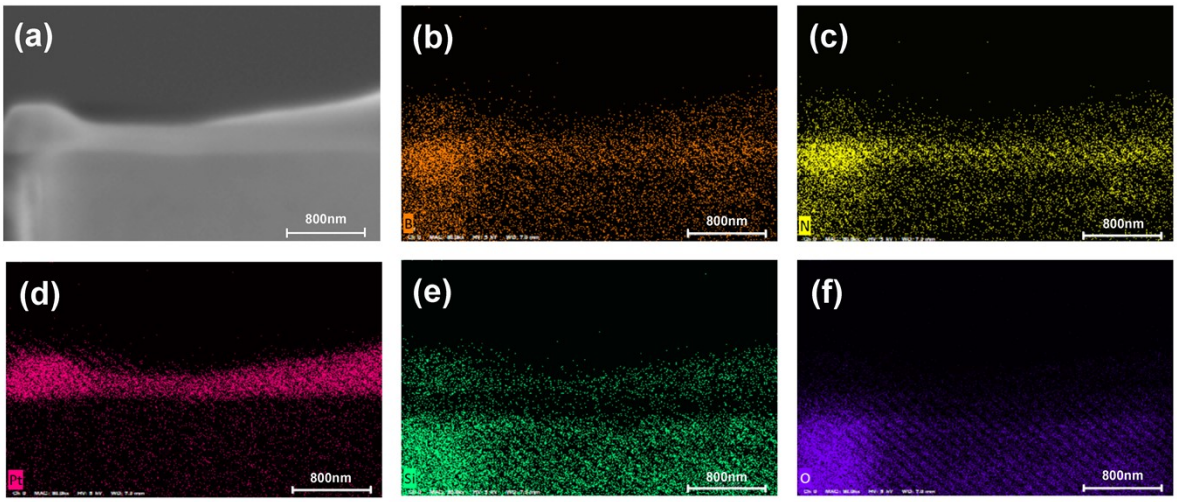

Figure S6. The image of the cross-section of h-BN film on a quartz substrate (a) and the corresponding EDS mapping of elements (b-f).

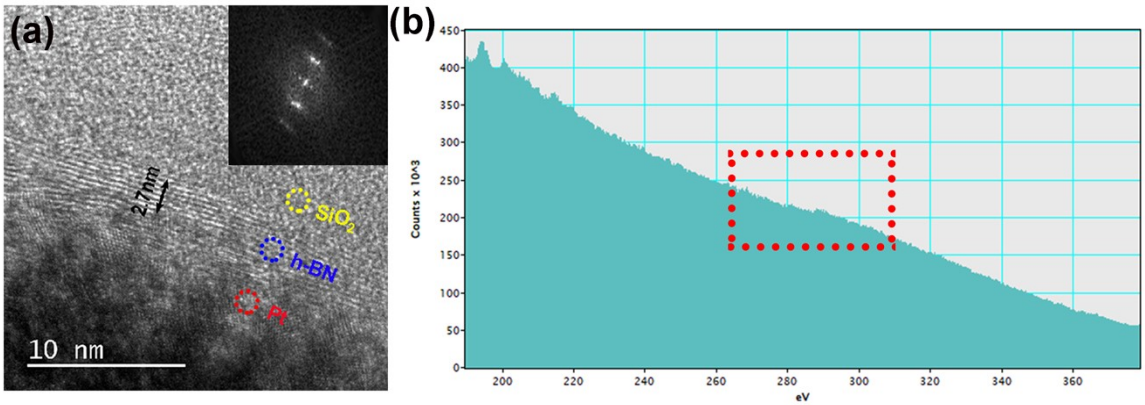

Figure S7. (a) HRTEM images of the cross-section of h-BN film grown on SiO_2/Si substrate. The fast Fourier transform (FFT) pattern is displayed in the inset. (b) EELS spectrum of the sample.

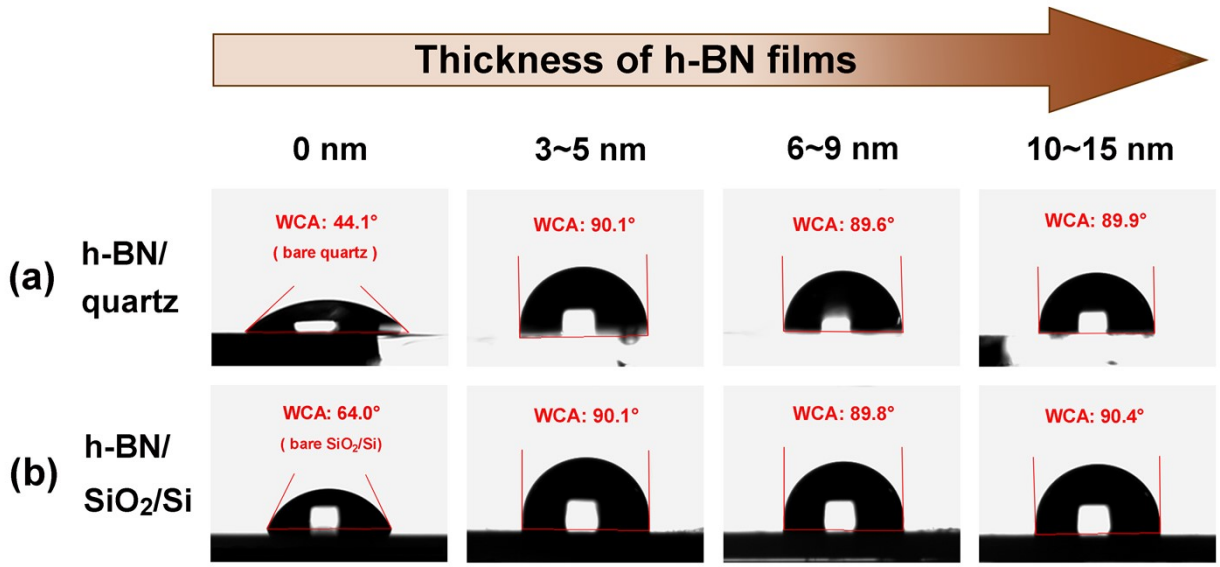

Figure S8. Water contact angle of multilayer h-BN grown on quartz substrate (a) and SiO_2/Si substrate (b).

The wettability is an important feature of a solid surface, which is determined by the chemical composition and microscopic geometric structure of the surface. Figure S8 shows the water contact angle of the surface of two bare substrates and h-BN films grown on the two substrates. We can see that although the water contact angle values of the two bare substrate surfaces show a large difference，a multilayer h-BN coating can switch the contact angles to a narrow range of 89.5°~90.5°. It reveals no matter what the water contact angle value of the bare substrate is, the surface of the grown h-BN film exhibits almost consistent WCA values independent of film thickness.

Discussion of growth mechanism

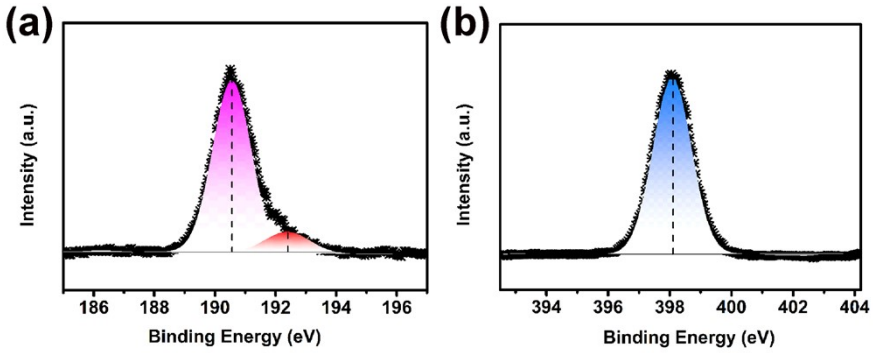

Figure S9. B 1s and N 1s core levels of the h-BN film.

The bonding state and the elemental composition of boron (B) and nitrogen (N) is investigated by X-ray photoelectron spectroscopy (XPS). From the Figure S9a we observed that the h-BN film has two types of B 1s core-level peaks at 190.5 (attributed to B−N) and 192.2 eV (attributed to B−O). Actually B-O bond formation plays an important role for the lateral growth of h-BN film. Figure S9b represents the N 1s peak at 398.1 eV for the N−B bonding. Furthermore, no B-C and N-C bonds were observed in the XPS measurements, indicating that a B-C-N phase had not been formed. B and N atoms were found to be almost in 1:1 ratio as measured by quantitative analysis of XPS spectra. These results evidently confirm growth of high quality h-BN crystals and continuous film on quartz substrate.

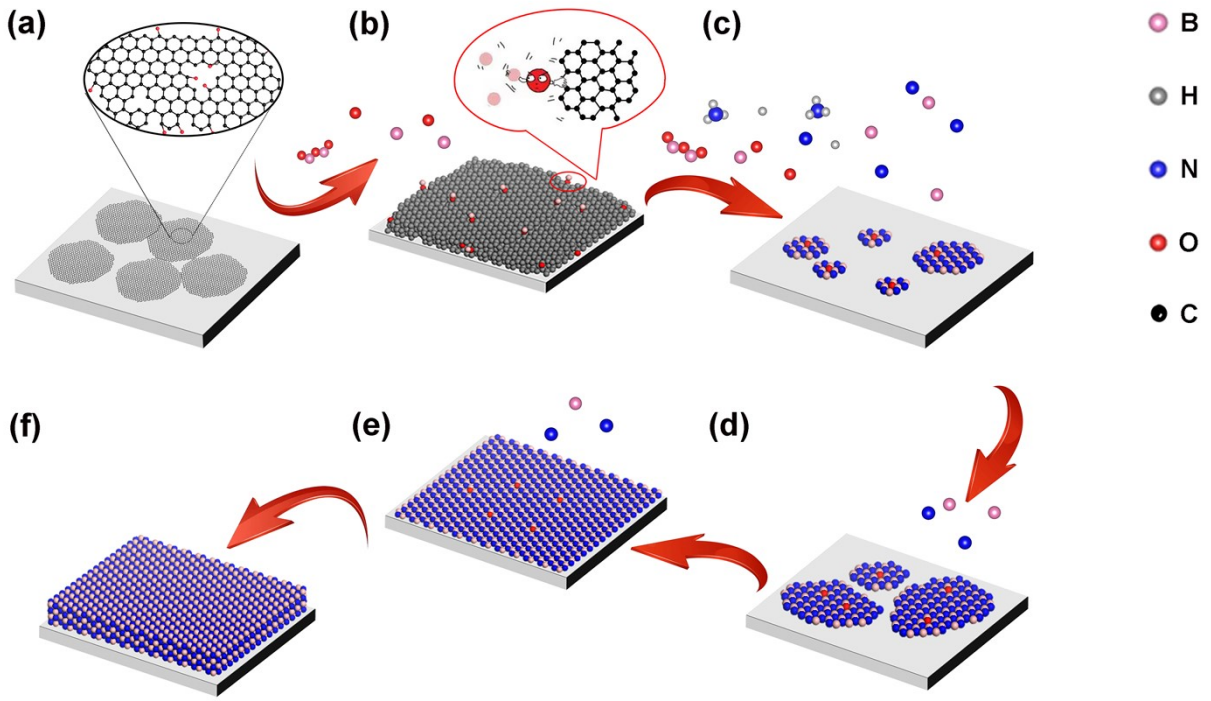

Figure S10. Schematic diagram of the reaction mechanism of h-BN films.

Generally, the direct growth of h-BN on dielectric substrates is extremely difficult due to the fact that these substrates are normally limited in catalytic activity. In our case with the assistance of rGO as seeding layer, high quality multilayer h-BN was directly grown on dielectric substrates at 850 ^{o}C, lower than those on metallic substrates, which is more favorable for the semiconductor industry. As is known, rGO is rich in disordered defects, step edges and oxygen related functional groups, which are all favored for h-BN nucleation. When rGO is pre-covered on the dielectric substrate, which are usually poor in activity, the high density of boundaries generated by the stacking of rGO layers and the inherent defects of rGO can be used as nucleation sites for h-BN film growth. More importantly, an ideal density of C-O dangling bonds on rGO surface (Figure S10a) are beneficial to

the adsorption of B atoms to form O-B-N bonds (see Figure S10b), that facilitates to the nucleation of h-BN when B- and N- containing vapors firstly arrive (Figure S10c).[2] The oxygen-assisted nucleation of h-BN film is also apparent from the XPS spectrum for B 1s. On the other hand, the concentration of rGO, that is the density of defects and fresh edges, will affect the growth of thicker h-BN films. The higher concentration of rGO will lead to a higher density of edges created by the stacking of rGO, which can provide relatively more nucleation sites, resulting in the rapid formation of continuous h-BN films in a relatively shorter time and grow vertically at the same time.

At a temperature of 850 °C, B_2O_3 and NH_3 molecules dissociate into B and N radicals, which may diffuse along the substrate surface. Meanwhile, the introduction of NH_3 provides not only sufficient active nitrogen species, but also hydrogen, which may facilitate the enhancement of the h-BN growth due to the H-induced etching and edges passivation.[3] If the rate of attachment of boron radicals and nitrogen radicals at the edge of h-BN domain is higher than the rate of their detachments, then the h-BN domains start to increase laterally in size (Figure S10d). Once the distance between any two nuclei reduces within a critical distance, they will move toward each other and coalesce into a single layer (Figure S10e).[4] As the arrival of the source vapors, the subsequent growth continues, resulting into more complex film shape. Eventually, a network of interconnected layer growth sequence occurs (Figure S10f). Meanwhile, once the rGO initials the nucleation of h-BN, the carbonous remains will be decomposed under 850 ^{o}C. The initial nucleation occurs in a very short time scale. On the other hand, if too much rGO centration in the seedling layers, for instance 1

mg/ml in this case, it will be left beneath the final h-BN films due to fast nucleation and subsequent growth of h-BN layer covering the excessive rGO.

From the comparative experiments in Figure 3, it can be seen that there is almost no formation of BN domains on the substrate without rGO covering on the surface, while the island-like BN domains appear on the substrate covered with a perfect graphene layer. This is because the perfect large-area high quality CVD graphene monolayer has a lower defect density and a longer diffusion length such that boron and/or nitrogen atoms tend to accumulate along the graphene edges. It is difficult to form a continuous h-BN film on such perfect graphene surface due to lack of sufficient BN domains. These results illustrate an important point that h-BN is more preferentially nucleated along graphene edges than bare SiO_2 surface. In fact, the growth of monolayer crystalline h-BN from fresh edges of monolayer graphene on Cu foils has been also demonstrated.[5] Compared with graphene, rGO with abundant defects and functional groups is more favorable for the nucleation and growth of h-BN films at relatively low temperatures. The higher growth temperature might increase the atom diffusion mobility, which is favor to form the h-BN layered growth on CVD graphene surfaces with lower density of defects.[6] In our case, the low growth temperature such as 850 ^{o}C obviously resulted into only the formation of tiny h-BN single crystal domains rather than continuous films on the graphene-covered substrate surface. Further work is planned to explore this growth process in more detail.

References

1. O. L. Krivanek, M. F. Chisholm, V. Nicolosi, T. J. Pennycook, G. J. Corbin, N. Dellby, M. F. Murfitt, C. S. Own, Z. S. Szilagyi, M. P. Oxley, S. T. Pantelides and S. J. Pennycook, *Nature*, 2010, **464**, 571-574.
2. F. Liu, T. Wang, Z. Zhang, T. Shen, X. Rong, B. Sheng, L. Yang, D. Li, J. Wei, S. Sheng, X. Li, Z. Chen, R. Tao, Y. Yuan, X. Yang, F. Xu, J. Zhang, K. Liu, X.-Z. Li, B. Shen and X. Wang, *Adv. Mater.*, 2022, **34**, 2106814.
3. H. Wang, X. Zhang, J. Meng, Z. Yin, X. Liu, Y. Zhao and L. Zhang, *Small*, 2015, **11**, 1542-1547.
4. R. Y. Tay, M. H. Griep, G. Mallick, S. H. Tsang, R. S. Singh, T. Tumlin, E. H. T. Teo and S. P. Karna, *Nano Lett.*, 2014, **14**, 839-846.
5. L. Liu, J. Park, D. A. Siegel, K. F. McCarty, K. W. Clark, W. Deng, L. Basile, J. C. Idrobo, A.-P. Li and G. Gu, *Science*, 2014, **343**, 163-167.
6. H. Arai, T. Inoue, R. Xiang, S. Maruyama and S. Chiashi, *Nanoscale*, 2020, **12**, 10399-10406.